

4

GL-TR-89-0231

Feasibility of Millimeter-Accuracy Geodetic
Positioning and Vehicle Tracking
With Repeater Satellites

Laureano Alberto Cangahuala

Massachusetts Institute of Technology
77 Massachusetts Avenue
Cambridge, MA 02139

27 July 1989

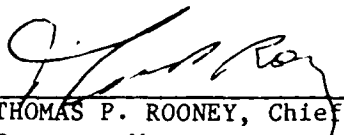
Scientific Report No. 5

APPROVED FOR PUBLIC RELEASE; DISTRIBUTION UNLIMITED

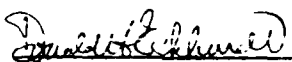
GEGPHYSICS LABORATORY
AIR FORCE SYSTEMS COMMAND
UNITED STATES AIR FORCE
HANSOM AIR FORCE BASE, MASSACHUSETTS 01731-5000

DTIC
ELECTE
NOV 24 1989
S B D

This technical report has been reviewed and is approved for publication.


THOMAS P. ROONEY, Chief
Contract Manager
Geodesy and Gravity Branch

FOR THE COMMANDER


DONALD H. ECKHARDT, Director
Earth Sciences Division

This report has been reviewed by the ESD Public Affairs Office (PA) and is releasable to the National Technical Information Service (NTIS).

Qualified requestors may obtain additional copies from the Defense Technical Information Center. All others should apply to the National Technical Information Service.

If your address has changed, or if you wish to be removed from the mailing list, or if the addressee is no longer employed by your organization, please notify GL/IMA, Hanscom AFB, MA 01731-5000. This will assist us in maintaining a current mailing list.

Do not return copies of this report unless contractual obligations or notices on a specific document requires that it be returned.

UNCLASSIFIED

SECURITY CLASSIFICATION OF THIS PAGE

REPORT DOCUMENTATION PAGE

1a. REPORT SECURITY CLASSIFICATION UNCLASSIFIED			1b. RESTRICTIVE MARKINGS N/A	
2a. SECURITY CLASSIFICATION AUTHORITY			3. DISTRIBUTION / AVAILABILITY OF REPORT Approved for public release; distribution unlimited.	
2b. DECLASSIFICATION / DOWNGRADING SCHEDULE				
4. PERFORMING ORGANIZATION REPORT NUMBER(S)			5. MONITORING ORGANIZATION REPORT NUMBER(S) GL-TR-89-0231	
6a. NAME OF PERFORMING ORGANIZATION Massachusetts Institute of Technology		6b. OFFICE SYMBOL (If applicable) Room 37-552	7a. NAME OF MONITORING ORGANIZATION Geophysics Laboratory	
6c. ADDRESS (City, State, and ZIP Code) 77 Massachusetts Avenue Cambridge, MA 02139			7b. ADDRESS (City, State, and ZIP Code) Hanscom Air Force Base, MA 01731-5000	
8a. NAME OF FUNDING / SPONSORING ORGANIZATION Geophysics Laboratory		8b. OFFICE SYMBOL (If applicable) GL/LWG	9. PROCUREMENT INSTRUMENT IDENTIFICATION NUMBER F19628-86-K-0009	
8c. ADDRESS (City, State, and ZIP Code) Hanscom Air Force Base, MA 01731-5000			10. SOURCE OF FUNDING NUMBERS	
			PROGRAM ELEMENT NO. 61102F	PROJECT NO. 2309
			TASK NO. G1	WORK UNIT ACCESSION NO. BN
11. TITLE (Include Security Classification) Feasibility of Millimeter-Accuracy Geodetic Positioning and Vehicle Tracking With Repeater Satellites				
12. PERSONAL AUTHOR(S) Cangahuala, Laureano Alberto				
13a. TYPE OF REPORT Scientific No. 5		13b. TIME COVERED FROM 86 Apr TO 89 July		14. DATE OF REPORT (Year, Month, Day) 1989 July 27
15. PAGE COUNT 24				
16. SUPPLEMENTARY NOTATION This report is an extension of AFGL-TR-89-0031. More attention is given to vehicle tracking, and to the selection of frequencies for minimum total transmitted power.				
17. COSATI CODES			18. SUBJECT TERMS (Continue on reverse if necessary and identify by block number)	
FIELD	GROUP	SUB-GROUP	Satellite geodesy, satellite positioning, satellite communications, repeater satellites, space geodesy, radio positioning, radio interferometry, radio tracking	
08	05	--		
19. ABSTRACT (Continue on reverse if necessary and identify by block number) A proposed satellite system (named "GeoBeacon") can detect and locate transmitters of a geodetic positioning system as well as transmitters of an emergency search and rescue (SAR) system. Simple, low-power transmitters on the Earth's surface will broadcast code-modulated signals. These signals will be received and rebroadcast to a processing site by a constellation of repeater satellites. A SAR transmitter can transmit at one frequency. For geodetic applications, a transmitter must transmit signals at more than one frequency, including a relatively low (e.g. 100 MHz) and a relatively high (several GHz) frequency. The low frequency signals would aid the acquisition and tracking of the higher frequency signals. By virtue of this aiding, the transmitted power required to enable tracking of signals at 10 GHz is about 100 times less than the power needed for tracking such a signal alone. Uplink power requirements both for aided tracking and for unaided acquisition are calculated as functions of frequency from 100 MHz to 50 GHz. The chief uncertainty in the calculations concerns the man-made radio noise environment in earth orbit. An algorithm is developed for the selection of frequencies by which aided tracking of the highest frequency signal can be maintained. This algorithm is based on a stochastic description of the kinematic and ionospheric contributions to the received signal frequencies and phases. Discrete Kalman filter equations are derived for estimating the covariance of phase and frequency estimates. Frequency selections and corresponding power budgets are presented for a vehicle-tracking/SAR system and for a geodetic positioning system.				
20. DISTRIBUTION / AVAILABILITY OF ABSTRACT <input type="checkbox"/> UNCLASSIFIED/UNLIMITED <input checked="" type="checkbox"/> SAME AS RPT. <input type="checkbox"/> DTIC USERS			21. ABSTRACT SECURITY CLASSIFICATION UNCLASSIFIED	
22a. NAME OF RESPONSIBLE INDIVIDUAL Dr. Thomas P. Rooney			22b. TELEPHONE (Include Area Code) (617) 317-3486	22c. OFFICE SYMBOL GL/LWG

INTRODUCTION

The tool that has most advanced man's positioning capability is the satellite. By positioning we refer to a broad range of applications that satellite positioning systems have made more accurate and reliable. For instance, positioning includes traditional construction surveying (e.g., for buildings, highways) as well as the development of large scale geodetic networks for boundary determination, aerial radar mapping, and gravity field measurements. Detection of local position changes (e.g., mining subsidence, structural deformation) and of changes more global in scale (e.g., plate tectonics, volcano growth) can also be monitored by satellite positioning systems. Also, since line-of-sight contact is not needed between sites, satellite positioning can aid in monitoring the location of large fleets of taxi cabs, trucks and railcars.

In general, the introduction of satellites to geodesy has brought with it many advantages over traditional land surveying techniques. First, since visual contact is not needed between measurement sites in satellite geodesy, the allowable area of investigation is virtually unlimited over the Earth's surface. Not only does the coverage area increase, but the number of man-hours needed per unit baseline distance is less than that required with line-of-sight surveying. Also, satellite receivers can be left at remote locations, whereas measuring these same sites with conventional methods requires the physical and computational effort of repeated visits to many sites for measurements. Finally, with worldwide coverage available through one system, all recorded locations can be tied to one global coordinate frame and one data base, thereby eliminating the difficulties involved in relating results from independent surveying campaigns.

Besides geodesy, positioning also includes navigation applications. For aircraft, ships, and spacecraft, this can include *en route* navigation, inertial navigation system updating, and precision maneuvers and approaches. Recreational users of satellite positioning systems can include pleasure boaters, mountain climbers, and eventually, auto drivers navigating through unfamiliar roads. Spacecraft in low earth orbit can use other positioning satellites for docking, radar imaging, or remote sensing. Positioning systems can also aid any these forms of transportation by monitoring for emergency distress beacons.

In addition to the possibilities of positioning systems mentioned, military applications include target and remotely operated vehicle position acquisition and tracking, as well as missile guidance, command, and control.

Overview of Extraterrestrial Positioning Systems

Before the existence of artificial satellites, extraterrestrial positioning techniques were based on astronomy, using a theodolite or sextant. The first satellite positioning systems were primarily used to improve the knowledge of the Earth's shape as well as the satellite's orbit parameters. This was accomplished by measuring the Doppler shift of the satellite's beacon. These early experiments evolved into the TRANSIT system, which began operation in 1961. In this positioning scenario, the user receives orbit information from ranges transmitted by 6 satellites in 1100 km circular polar orbits. The user can compute his position by integrating the measured frequency shifts and using the transmitted orbit data.

A second satellite system which operated on measured Doppler shifts began in 1978. Argos was a cooperative project among the French Centre National d'Etudes Spatiales (CNES), NASA, and the U.S. National Oceanic and Atmospheric Association (NOAA). The Argos user transmitted a signal at 401.65 MHz, which was received by a TIROS/N - class weather satellite, which then repeated the signal back to one of three tracking stations. All received signals were relayed to a central data processing center in Toulouse, France. Afterwards, the processed position and velocity results were mailed to the user. Accuracies of 3 km (3σ) and 0.5 m s^{-1} (3σ) were claimed in position and velocity, respectively. The system could handle up to 4000 transmitters simultaneously, assuming an even distribution of sites over the Earth's surface.

Another system that operates in a manner similar to Argos is the COSPAS-SARSAT search and rescue (SAR) system, a venture involving Canada, France, the United States and the Soviet

Union. So far, the program has been responsible for saving over 1150 lives as of the fall of 1988. The success of COSPAS-SARSAT has led the federal government to require that all boats carry a SARSAT emergency transmitter by 1989. These transmitters operate at civil and military distress frequency allocations (121.5 MHz, 243 MHz), and their signals are eventually picked up by one of 5 satellites in the COSPAS-SARSAT system. The transmitter, sending a 120 s signal every 50 s, runs on a peak power of less than 100 mw, and costs as little as \$150 in 1988 according to an advertisement in *Guns and Ammo* magazine.

Currently, the most widely used satellite positioning system is the NAVSTAR (NAVigation Satellite Time And Ranging) Global Positioning System, hereafter referred to as GPS. When fully deployed in the mid- to late-1990's, the GPS will consist of: 18 (7 as of late 1988) satellites in 12-sidereal hour circular orbits; a ground-based control system to synchronize the satellites, update their broadcast messages, and monitor their health and orbits; and user receivers, which will acquire and track the signals from GPS satellites in view. A GPS receiver can distinguish between different satellites by either the coded modulation of the signal from each satellite or by having prior estimates of the satellite orbits and the Doppler shifts of the received signals. Position can be determined by measuring the group delay of the modulation and/or the phase delay of the carrier.

Capabilities and Limitations of GPS

Of all the positioning systems in use or in active development, GPS in principle holds the most promise for the wide range of needs of the scientific and commercial communities. For example, through advances in signal processing and in orbit determination, GPS has made possible relative measurements over distances of the order of 2000 km with an accuracy on the order of 1 cm. By using quasar signals instead of satellite signals, the movements of some of the Earth's crustal plates have already been accurately mapped; these measurements are being repeated and extended with GPS. GPS can also be used to monitor the structural dynamics of dams, offshore oil drilling platforms, or the ground over areas of mining or water or oil removal.

Although poor satellite geometry may cause the fully operational GPS to suffer periodic degradation of performance, its accuracy already exceeds that of any navigation system in operation today. With the accuracy of the GPS and the reliability of the terrestrial LORAN system, a Hybrid GPS/Loran system could become a powerful aviation navigation tool.¹⁷

In applications where position and velocity measurements are needed at many sites, however, using GPS brings up a problem of cost. In many of these applications, a project's success depends on how many locations (or objects) can be located and tracked at once. Except in studies where measurement sites are less than about 100 m apart, (e.g., in dam deformation), every location will require its own GPS receiver. Although the market prices of receivers should drop as the remaining GPS satellites are placed into orbit, the price of a receiver alone is currently on the order of \$50,000 (1988 dollars). At these prices, these receivers can not be left unattended at sites where vandalism would be a problem. These costs make it prohibitive for any institution to perform measurements at more than tens of locations, or hundreds if the manpower needed to move dozens of receivers from point to point is available.

In any case, the required follow-up work for each campaign gives rise to a second problem. Specifically, there must also be a means for the data generated in all the receivers to be brought together. This would require additional visits to each receiver or the addition of another system to transmit the receiver data to a central processing site. A third problem is that the high power demands of geodetic receivers (at 20-200 w apiece) make it cumbersome for them to be self-powered by solar cells.

Motivation for a New Satellite Positioning and Tracking System

One method of circumventing the problems outlined above has been suggested by Prof. Charles Counselman. Small radio beacons each transmitting several frequencies are set up at the survey points, and a constellation of repeater satellites receive the signals (see Figure 1 for an

overview of the system, nicknamed "GeoBeacon"). All the received signals are then relayed to a central site where the processing is done for the entire network of transmitter sites. The first advantage of this scheme over the GPS positioning methodology, is that transmitters are cheaper than GPS receivers. These transmitters could be sold for relatively low prices, as are the SARSAT emergency beacons for outdoorsmen that were mentioned earlier. The GeoBeacon transmitter would need only a crystal oscillator to achieve the necessary frequency stability, and a means for "tagging" each transmitter's carrier signal with coded modulation. If the required uplink transmitter power were low enough, these transmitters could be powered by solar cells and left at their respective sites without any return visits or maintenance checks. The second advantage of the system is that if a particular transmitter's signal (identified by its code) should no longer be received by the satellites, it can be replaced more cheaply than any GPS receiver could. This combination of 'throwaway' transmitter, brought by its lower cost, and the freedom from repeated visits to each measurement site should make it possible to monitor tens or hundreds of thousands, instead of hundreds, of locations.

What other possible uses does this system offer? Since the measurements are made and results are obtained at a central site, real time results for most users may not be practical. This system is not intended to replace GPS, but its different arrangement opens the opportunity for applications other than cheaper geodetic measurements. Anything can be tracked so long as a transmitted signal can be received by the observing constellation of satellites. For instance, with pseudo-random codes used to minimize detection by an enemy, the system could be used to track troop movements. Transmitters could be timed to transmit only at certain times in order to minimize the possibility of detection, or to take advantage of energy sources (e.g. the moving wheel of a car, the ignition of a motor, etc.) Although few applications require the precision of geodetic measurements, this new system can be designed with geodetic level accuracy as its primary goal, and still allow the opportunity of tracking other objects. Unlike GPS, the GeoBeacon can furtively monitor objects, which could be an asset to surveillance groups. By giving each transmitter a unique coded message, one could recover the positions of all transmitters, and distinguish transmitters of different projects. Therefore, this system could simultaneously perform geodetic measurements and track an emergency beacon from a mountain climber.

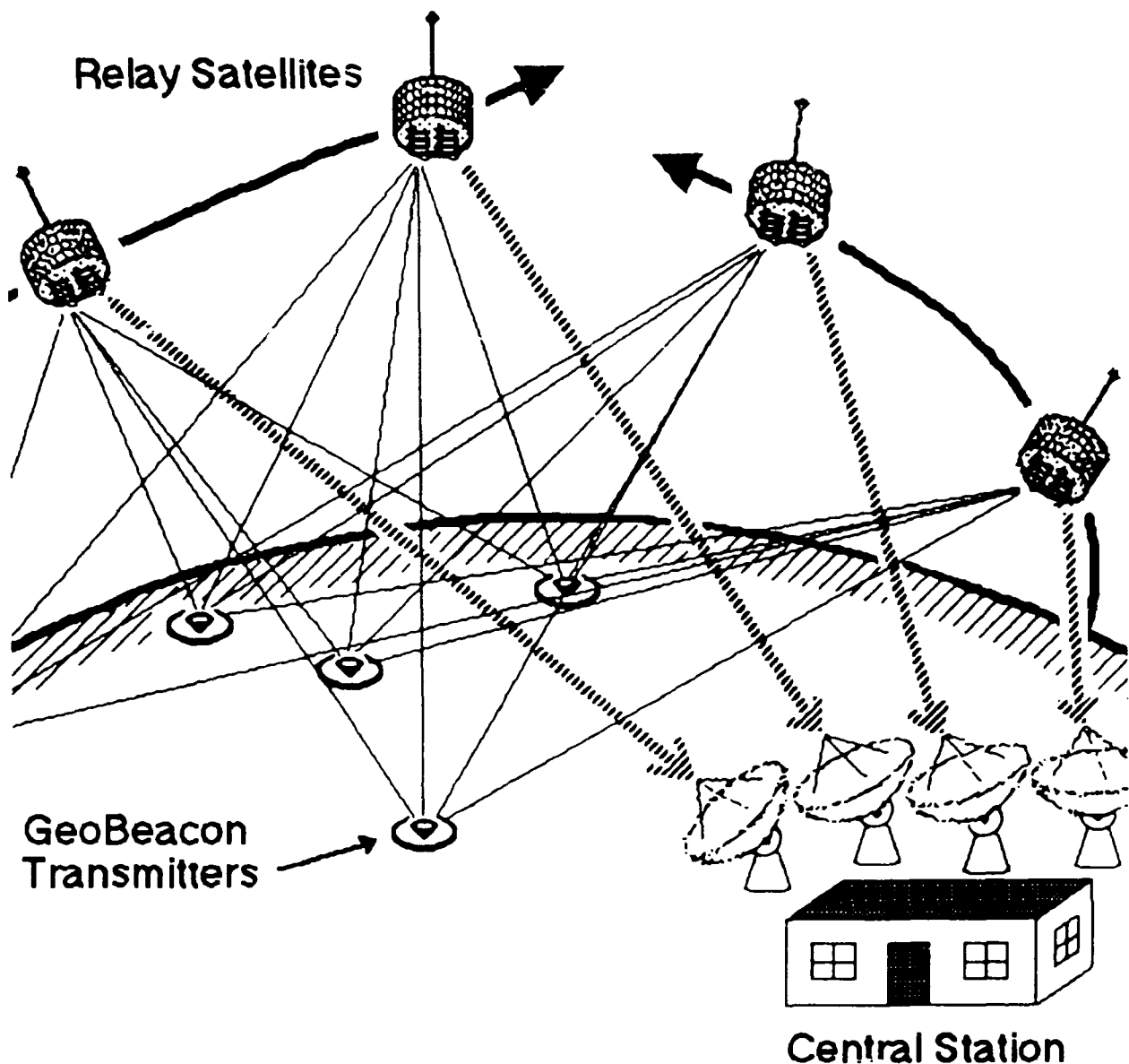


Figure 1. Overview of "GeoBeacon" Satellite Positioning System

In addition to these positioning projects, this new system could make it possible to monitor electron concentrations throughout different slices of the ionosphere, which could aid in ionospheric studies. Knowledge of this ionospheric contribution would aid in processing data for this system or any other satellite positioning system (including GPS).

These practical tracking, positioning, and measuring opportunities, which are physically and economically unattainable by GPS alone, will make this satellite positioning system worthwhile and cost effective. Therefore, this study will address the feasibility of using a low-power transmitter operating at several selected frequencies for locator and tracking purposes. This study will focus on the estimation of the required transmitter power and the frequency selections which would provide effective service for the applications mentioned.

The following section outlines the assumed needs of the users of the new system, introduces a possible orbit configuration for the satellite constellation, and reviews some parts of a radio positioning system. The power budget section examines the requirements of the radio link

(e.g., SNR, antenna gains) and relates them to the transmitter power need for the uplink. The objective of this section is to effectively demonstrate to a system designer what factors predominate the uplink power requirements for signal acquisition and tracking at different frequencies. The frequency selection segment reviews the models and assumptions used for choosing the system frequencies. The goal of this section is to provide an algorithm for the system designer to follow in selecting the desired frequencies, such that information obtained from measurements at each frequency is being used to the fullest in acquiring and tracking signals at other frequencies. Following these discussions are an analysis of results and conclusions for the estimated transmitter power and frequency selection method. Finally, this study includes suggestions for improving the models used and a possible experiment to simulate this positioning system.

DEVELOPMENT OF PROTOTYPE SYSTEM DESIGN

Definition of User Needs

Although it is not possible to anticipate the performance requirements of every user of this new system, for this feasibility study their needs will be divided into two groups. One group will not require precision positioning, but instead will need positioning updates at intervals on the order of an hour or less and most importantly, the lowest possible transmitter power. Locator systems such as a SAR network would be an application with these needs. The second group will have a high precision positioning requirement (1 part in 10^9 accuracy in baseline measurements), but may only require updates on the order of once a month. These are the needs of a crustal motion project.

To fulfill the requirements of both groups, a wide range of frequencies must be used in the positioning system. The lower limit on frequency selection arises from the increasing possibility that the uplink signal will become totally reflected by the ionosphere as transmitter frequency decreases. Therefore, a lower frequency bound of 100 MHz is assumed for this study. While frequencies between 100 MHz and 1 GHz have proved to be effective for SAR missions, ionospheric phase scintillation at frequencies below 1 GHz makes phase prediction and tracking difficult. The precision in satellite geodesy comes from tracking the carrier phase instead of the transmitted code. Also, position determination precision tends to increase with shorter wavelengths, as will be shown. Therefore, frequencies above 1 GHz must also be considered for performing geodetic measurements.

The strategy by which both types of services will be performed is as follows. The lowest frequency will most likely be the selection used for SAR. In addition to this role, signals acquired at this frequency allocation will be used to predict the frequency shift of signals received at the next higher frequency. Once the second frequency is tracked, information from both frequencies will be used to acquire and track the signal at the next highest frequency, and so on. After frequency selections exceed 1 GHz, both frequency and phase predictions of the signal will be made, for it is the phase measurements of frequencies above 1 GHz which are relevant for precise geodesy.

Possible Satellite Constellations

Since the intent of this system is to provide positions for thousands of sites in a manner unattainable by GPS, it is conceivable that both systems could be merged on a future generation NAVSTAR/GPS satellite. The positioning and ionospheric measuring capabilities of this new system would be of interest to the military. In addition, with projected lifetimes of current navigation systems such as Omega reaching 2005 [19], GPS can be expected to have a operating lifetime over several generations of GPS satellites. With that scenario in mind, the design will assume a GPS-style constellation of 18 repeater satellites orbiting at an inclination of 55 degrees in 12-sidereal hour orbits.

or	<input checked="" type="checkbox"/>
	<input type="checkbox"/>
	<input type="checkbox"/>

Distribution/	
Availability Codes	
Dist	Avail and/or Special

A-1

GeoBeacon Transmitter

One objective of this system is to provide a relatively inexpensive means of positioning and/or tracking of thousands of sites. As mentioned earlier, by having transmitters instead of receivers at the sites of interest, the need to visit individual sites to recover information in receiver memory is eliminated. This lowers the number of man-hours needed to conduct large surveying campaigns. The system is meant to minimize transmitter power and frequency stability requirements. With a total power requirement on the order of a watt, these site transmitters can run on solar cells charging a battery pack. The design calls for a crystal oscillator to be used as a frequency standard, as with the emergency transmitters used in the SARSAT system. Higher-stability frequency standards, such as an atomic standard, will only be required at the central processing sites.

With their energy self-sufficiency and low cost, these transmitters can be considered disposable. That is, once the transmitter's working lifetime is exceeded, it can be replaced without burdening the resources of the user. For the geodetic user, the transmitter can be considered a cheap source of frequency and phase by which site location can be determined. For the vehicle tracker, the transmitter can be considered a cheap source of coded signals. Since every transmitter could be given its own individual wideband (~1 MHz) pseudo-random code, unauthorized detection and/or jamming, as well as unintentional interference can be avoided.

Signal Processing and Measurement Resolution

The objective of a coded signal receiver is to distinguish the signal of a selected transmitter from the signals of other transmitters. Once the signals are separated, phase measurements are made. The details of making a measurement, as well as techniques such as double differencing, will not be covered here.¹² Position is determined from these phase measurements, and one cycle of phase corresponds to one wavelength of distance in position. Phase measurement accuracy is typically a few percent of a cycle. Therefore, in order to obtain greater geodetic precision, transmitter frequencies need to be as high as possible.

POWER BUDGET

For this study, it is assumed that the receiving antenna for the downlink will be a dish with an effective aperture of about 1 m², and the satellite transmitting power will be about 1 w. Relative to the uplink, the downlink signal will have a much higher signal to noise ratio; therefore the study focused on the power budget for the uplink. The objective of this portion of the study is to investigate the uplink power required over the range 100 MHz - 50 GHz. As mentioned earlier, the lower frequency limit was selected due to the increasing possibility that the uplink signal would reflect off the ionosphere at lower frequencies. The upper limit was chosen since the required transmitter power is impractically high (as will be shown) at higher frequencies, and because there is no known need to use such short wavelengths. The uplink power budget defines the required power transmitted by the GeoBeacon at a particular frequency. For this study the equation defining the uplink power will be defined in dB notation for simplicity in examining each term:

$$P_T \Big|_{\text{dBw}} = \frac{P_R}{N} \Big|_{\text{dB}} + P_S \Big|_{\text{dBHz}} - G_T \Big|_{\text{dB}} - G_R \Big|_{\text{dB}} + P_L \Big|_{\text{dB}} \\ + L_a \Big|_{\text{dB}} + L_R \Big|_{\text{dB}} + M_{\text{sys}} \Big|_{\text{dB}} + I_P \Big|_{\text{dB}} + kT_{\text{sys}} \Big|_{\text{dBwHz}^{-1}} \quad (1)$$

P_T = Transmitter Power

$\frac{P_R}{N}$ = Uplink Signal to Noise Ratio (SNR)

B_S = Signal Bandwidth

G_R = Receiver Antenna Gain

L_a = Clear Atmosphere Transmission Loss

M_{sys} = System Margin (3 dB)

T_{sys} = System Noise Temperature

G_T = Transmitter Antenna Gain

P_L = Vacuum Path Loss

L_R = Rain Attenuation

L_P = Antenna Pointing Loss (3 dB)

k = Boltzmann Constant

Signal to Noise Ratio (SNR)

The accuracy of geodetic measurements made with the GeoBeacon system is proportional to the accuracy with which the highest frequency carrier phase can be tracked. In order to perform phase measurements with an accuracy of a few percent of a cycle, SNR needs to be at least 15 dB.

Integration Bandwidth

The integration bandwidth (B) is the inverse of the integration time span (t). Two sets of assumptions were made for integration bandwidth values as a function of frequency. First, for signal acquisition purposes, a value of 1 Hz was selected at 100 MHz. As will be shown in the discussion concerning frequency selection, as frequency increases, the kinematic effect upon phase increases relative to the ionospheric contribution. The integration bandwidth size will reflect the kinematic behavior as frequency increases. Since the relation of kinematics to phase is proportional to frequency, the acquisition bandwidth will increase linearly with frequency.

Bandwidths for Unaided Signal Acquisition and Aided Tracking

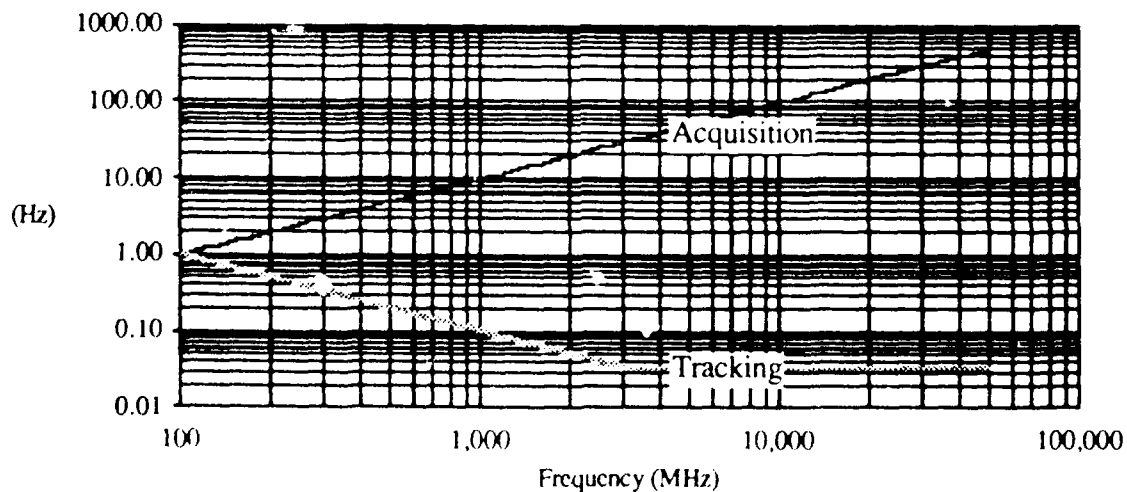


Figure 2. Integration Bandwidth

Once the signal is successfully acquired, the kinematic effect upon the phase has been (hopefully) cancelled out, leaving only the ionospheric effect to change the predicted phase. The contribution of this ionospheric process to phase is proportional to the inverse of frequency, so the bandwidth required for tracking decreases from 1 Hz at 100 MHz to 1/30 Hz at 3 GHz. At 3 GHz the integration time is 30 s, at which point the signal may leave the integration bandwidth during the integration time span. Therefore, the lower limit upon tracking bandwidth is set at 1/30 Hz for frequencies above 3 GHz.

Transmitter Antenna Gain

The transmitting antenna should illuminate the whole sky, but not the ground. An antenna which had uniform gain in the upper hemisphere and none in the lower would have an upper hemisphere gain of +3 dB. In practice, the gain of an antenna must taper smoothly as a function of elevation angle, so that a realistic gain for elevations above 20° is about -2 dB.

Receiving Antenna Gain

The receiving antenna is pointed at the Earth's center and its beam's main lobe is wide enough at the 3dB points to encompass transmitters the the satellites elevation angle is 20° . By geometry we can calculate this 3dB beamwidth (ϕ) and the corresponding boresight gain, assuming that the satellite altitude (h) is that of a standard GPS satellite, 19700 km. The minimum allowable elevation angle was chosen to be 20° because it is difficult to find many locations on the Earth's surface which allow a clear view of the sky at lower elevation angles. It also represents a tradeoff between the increased coverage area for each satellite gained with a lower minimum elevation angle and the decreased vacuum and atmospheric losses with a higher minimum elevation angle.

The receiver gain used for the power budget will be 3dB off the boresight gain, 13.3 dB.

Path Loss

The vacuum path loss calculations for our measurements are based on the longest possible uplink slant range, which occurs when a signal transmitted from the Earth's surface at an elevation angle of 20° to the satellite orbiting at an altitude of 19700 km. The path length (R) is found to be 23200 km. As a result of this path length assumption, the vacuum path loss is proportional to transmitter frequency squared.

Atmospheric Signal Attenuation

In the frequency range being considered for this design, the principal mechanism by which radio waves are attenuated is molecular absorption. In the Earth's atmosphere two major gases have resonance frequencies in the range of interest (100 MHz - 50 GHz), water vapor and oxygen. Global samples have been taken of the contributions of water vapor and oxygen towards radiowave attenuation as a function of temperature and surface water vapor concentration (humidity).¹⁰ The specific attenuation from these two gases can be calculated as a function of surface temperature and water vapor concentration. The integral of the specific attenuation over the entire slant path through the atmosphere yields the total atmospheric attenuation, which is a function of elevation angle. Estimates of the total zenith attenuation can also be calculated from a second set of coefficients derived from a regression analysis by Crane¹⁰. The resulting variation of atmospheric attenuation with respect to frequency is shown below. Note the effect of the water vapor resonance at 22.3 GHz and the oxygen resonance as 60 GHz is approached.

Atmospheric Attenuation

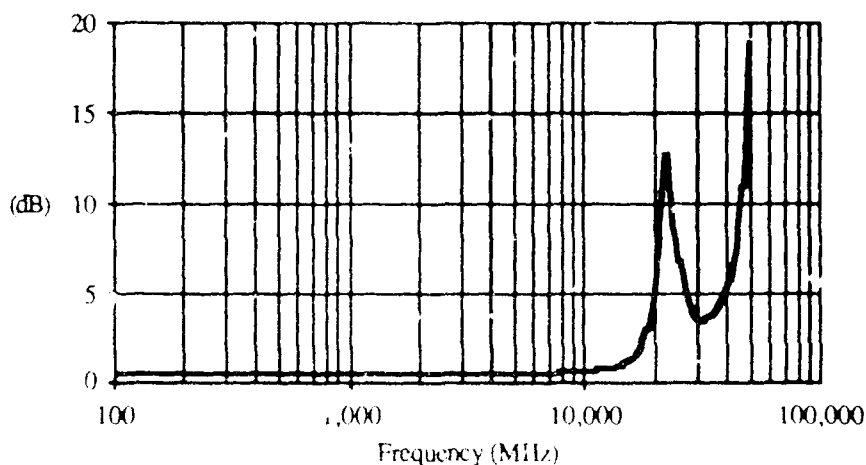


Figure 3. Total One-Way Atmospheric Attenuation (L_a)

Rain Attenuation

Attenuation of the uplink signal due to rain was not considered in the design. As shown in the previous section, rain attenuation is significant only at the higher frequencies being considered ($f > 20$ GHz). The most intense cases of precipitation have time spans on the order of a few hours and are localized in nature. Therefore, the geodetic capabilities of this system would not suffer appreciably. For the same reason, the system's emergency locator capability would hardly be diminished. For vehicle tracking purposes, however, the user would have to tolerate a service outages on the order of %0.01 of the year (10 hr).¹⁰ Since tracking results will not be generated in strictly real time under ideal weather conditions anyhow, performance degradation due to heavy precipitation is not focused on in this study.

System Noise Temperature

The effects of unwanted noise on the uplink show up in the system noise temperature (T_{sys}). The receiving antenna's 3 dB pattern will fall upon the Earth's surface, so the contributions to the noise temperature directly from the sun and from deep space will be neglected. The total noise contribution from the Earth comes from both natural and man-made sources. Due to a shortage of measurements of the radio frequency environment in Earth orbit, the estimates of natural and man-made noise carry the greatest uncertainty of any estimate in this study.

Natural and Man-Made Radio Sources. The natural radiative temperature of the Earth has basically two regimes. At frequencies below the resonances of water vapor and oxygen (~ 20 GHz), the Earth's surface temperature dominates, with an average value of 290 K. At higher frequencies, the atmosphere absorbs the surface thermal radiation and reradiates it, with an upper limit of 290 K.¹⁴ The value of 290 K is often used for antenna temperature in uplink noise calculations, although some consider values between 60 and 240 K to be more realistic.¹⁵ Since it is a conservative estimate, at frequencies where man-made noise power can be considered negligible, the noise temperature is assumed to be 290 K.

The contribution to the noise environment from man-made sources comes in two forms. One is accidental transmission from electrically powered machinery, hereafter referred to as

unintentional man-made noise. The second form is from transmitters deliberately operating (legally or illegally) in frequency allocations assigned to this new system. This noise will be referred to in this study as deliberate transmitter noise.

There is a growing need, which has been recognized by the international telecommunications community, to measure and control the amount of electromagnetic interference to radio links both on Earth and in Earth orbit. Since insufficient measurements of man-made radio emissions to outer space exist over the 100 MHz - 100 GHz range of the spectrum, estimates must be made of the expected noise level.

Most studies addressing this topic to date have assumed the satellite to be a communications satellite at a geosynchronous altitude. Since the main lobe of the satellite receiving antenna gain pattern in this design will also fall within the Earth disc, the results of these studies are relevant.

Unintentional Man-Made Noise A study conducted by Skomal¹³ assumed that the impulsive contributions to this incidental noise power $p_h(f)$ from consumer products, automotive ignition systems, industrial equipment and electric-power generation resembled thermal noise in nature at great distances. Skomal proposed that most unintentional man-made noise comes from metropolitan areas, and that their contributions can be modeled and summed to yield the total incidental noise power. The distribution of urban areas for the Western Hemisphere was tabulated, along with their characteristic dimensions.

The resulting estimated unintentional man-made noise power spectral density is shown in the figure below. This estimate assumes that the satellite is over North America; it is reasonable to believe that there is no other location over the Earth's surface where the level of interference noise will be greater.

Deliberate Transmitter Noise In a study conducted by Birch and French⁸, a compilation was made of all the power emitted from licensed transmitters over the frequency range 117-155 MHz. Their transmitter information sources included the IFRB (International Frequency Registration Board), the ECAC (Electromagnetic Compatibility Analysis Center), and Jeppesen Air Manuals. From this information a program was used to estimate the noise power density received by a geosynchronous satellite at a longitude where the expected noise power would be relatively high compared to other longitudes.

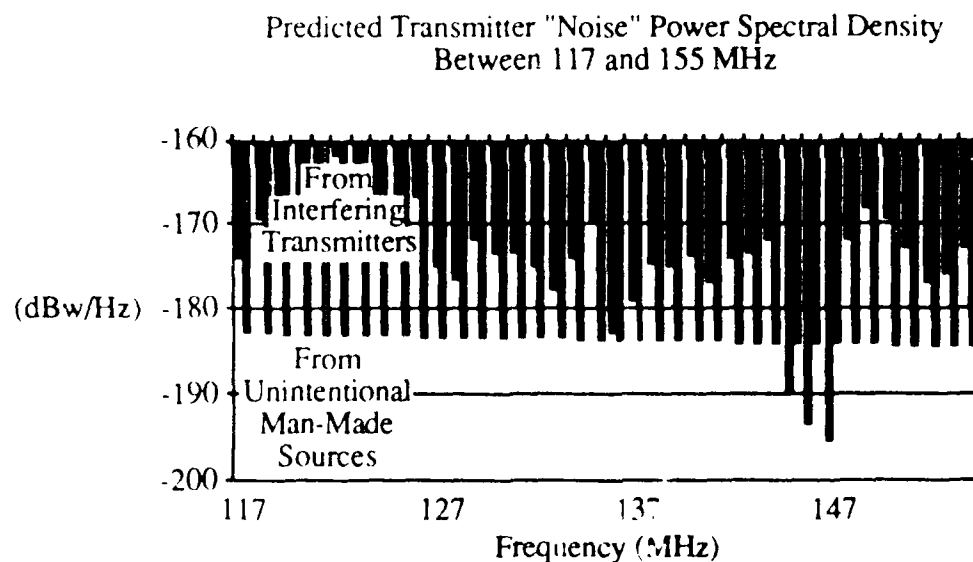


Figure 4. Predicted Transmitter Noise Power Density (from geosynch. orbit @143° W. Long.)

The frequency allocations of the frequency range in Figure 4 are listed below¹¹:

- | | |
|--|----------------------------------|
| 1) 117 - 118 MHz: Aeronautical Radionavigation | 6) 143 - 144 MHz: Space Research |
| 2) 118 - 136 MHz: Aeronautical Mobile | 7) 144 - 146 MHz: Amateur |
| 3) 136 - 137 MHz: Aeronautical | 8) 146 - 150 MHz: Fixed Service |
| 4) 137 - 138 MHz: Space-to-Earth | 9) 150 - 155 MHz: Fixed Mobile |
| 5) 138 - 143 MHz: Aeronautical Mobile Services | |

When the estimated incidental noise density is included with the predicted transmitter noise density, it appears that on the average man-made transmitter noise increases the noise density by 10 dB. When this system is implemented there is no guarantee that it will be allocated frequency bands with little interference noise, such as the amateur radio band (region 8 above). These predicted estimates will likely increase with time as the number of transmitters increases. As a result of these predictions, the man-made transmitter noise power density is assumed to be 10 dB above the level estimated from unintentional sources (see Figure 5).

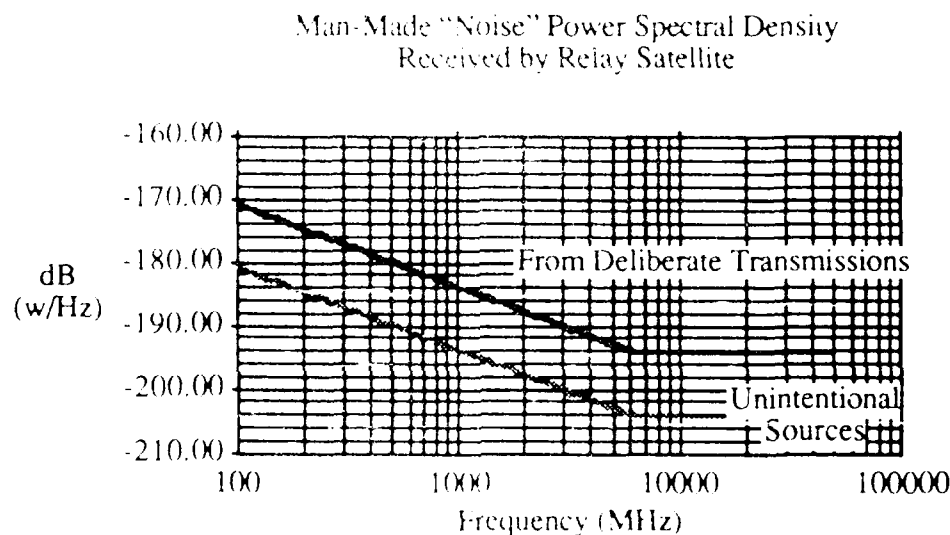


Figure 5. Total Man-Made Noise Power Density Assumption

International Frequency Allocation Need

No measurements of the actual radio noise levels from transmitters at GPS-orbit altitudes were available. However, one can calculate the amount of transmitter noise which can be tolerated at any particular frequency bandwidth. The estimates shown below demonstrate that the new system cannot share its frequency allocations with commercial radio broadcasters or microwave link users. Therefore, there may be a need to reserve frequency allocations for this new system, as was done for the COSPAS-SARSAT and GPS systems.

For the case of a satellite receiving interference from a ground transmitter, an interference-free link must satisfy the following power relation:

$$P_i \big|_{\text{dBw}} \geq P_e \big|_{\text{dBw}} + C_e \big|_{\text{dB}} + G_R \big|_{\text{dB}} + \frac{L F_r}{\Delta F_e} \big|_{\text{dB}} - P_L \big|_{\text{dB}} - D_p \big|_{\text{dB}} - A_b \big|_{\text{dB}} - D_f \big|_{\text{dB}} - A_h \big|_{\text{dB}} (\epsilon) \quad (2)$$

where

P_i = Permissible Interference Power Level (see Figure 5)

P_e = Power Transmitted from Interfering Transmitters

G_c = Transmitting Antenna Gain in direction in question

G_r = Satellite Receiver Antenna Gain in Direction in Question (13.27 dB)

$\frac{\Delta F_r}{\Delta F_e}$ = Receiving/Interference Bandwidth Ratio. (0 dB for most conservative case)

P_L = Vacuum Path Loss of Interfering Signal

D_p = Transmitter - Receiver Mismatch Polarization Losses (0 dB; most conservative case)

A_b = Receiver Connection Losses (0 dB; most conservative case)

D_f = Frequency Decoupling (0 dB; most conservative case)

$A_h(\epsilon)$ = Losses due to Horizon Relief (0 dB; most conservative case)

Two cases are considered: a commercial FM radio transmitter and a microwave relay link. At 10 kw per transmitter, this corresponds to 0.021 transmitters over the area in view, which is equivalent to a FM transmitter density of $8.75(10^{-5})$ transmitters per $10,000 \text{ km}^2$. Therefore, this new system could not coexist with commercial FM radio.

For the case of a microwave transmitter, this corresponds to 0.59 transmitters over the area in view, or a transmitter density of 0.34 transmitters per $10,000 \text{ km}^2$ (the assumed density is currently 5 transmitters per $10,000 \text{ km}^2$). Therefore, fixed radio-relay allocations would lend themselves more than the commercial FM band to the possibility of frequency sharing with this new positioning system. Nevertheless, the level of noise interference in this case is over 10 times the amount tolerable by the new system. There will be a need to study the feasibility of frequency sharing for the new system at other frequency allocations.

Power Budget Results

The total required power as a function of frequency is shown below, in addition to the total required power as a function of frequency. Note how the dependence of acquisition bandwidth upon frequency dominates the power requirements at lower frequencies. Once the signal is acquired at the lowest frequency, however, one can take advantage of the drop in ionospheric phase shifting as frequency increases. This decrease creates a slight drop in the power needed for the frequencies to be tracked, until atmospheric attenuation and vacuum path losses begin to dominate.

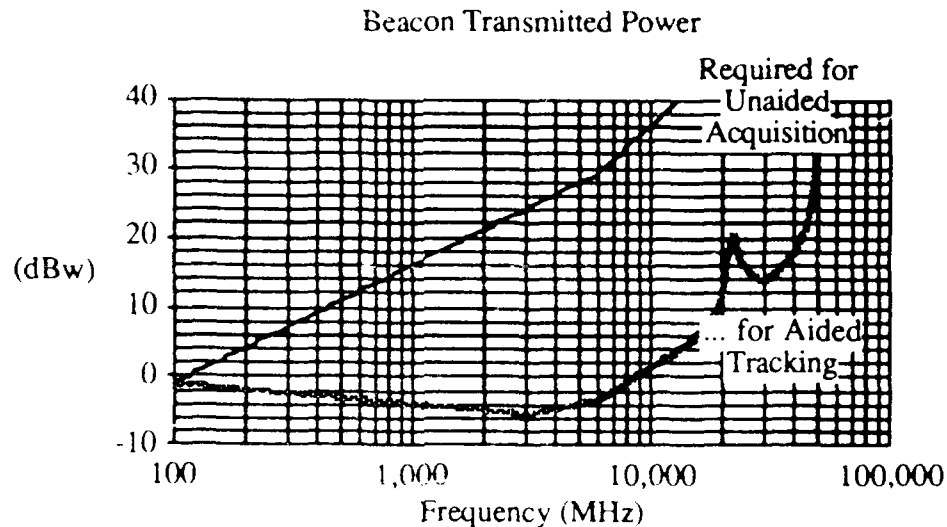


Figure 6. Uplink Power Budget

The fact that at frequencies under 9 GHz the required power for aided tracking is less than 1 w is encouraging. For a transmitter operating at a 10% duty cycle, broadcasting at 10 frequencies between 0.1 - 9 GHz, the average total power required is 1.0 w. If one wanted to make studies of the water vapor content of the atmosphere, one could add additional frequencies near the water vapor resonance (with the additional penalty in power required).

The calculated powers required for unaided acquisition and aided tracking reflect the contributions of many assumptions. One could transmit at less power than those dictated by Figure 6 to achieve other goals. For instance, one could measure water vapor content at the water vapor resonance at 22.5 GHz without necessarily having to track signal phase or frequency.

FREQUENCY SELECTION

As shown earlier, the precision of geodetic measurements improves with decreasing wavelength. One could perform high precision geodesy with a transmitter operating at one relatively high frequency ($f > 10$ GHz). However, it would require a prohibitively large amount of power to acquire and track the signal at this high frequency.

There is another method by which signals at high frequencies can be accurately tracked. Let the transmitter transmit signals at two frequencies, one high and one low, both being derived by multiplication from the same oscillator so that the ratio of the frequencies is a known constant. One first acquires and tracks the low frequency signal. Having measured the frequency of this signal, one multiplies the measured value by the known ratio to obtain a prediction of the higher received frequency. This prediction will have an error, due to (1) error of measurement of the lower frequency, and (2) ionospheric effects, which are not proportional to frequency. This prediction error limits how far up in frequency one can go and still expect to acquire a signal within one's tracking bandwidth. Measurements at this higher frequency may be used in acquiring a third frequency, and so forth, until one can acquire and track signals at frequencies necessary for geodetic work. The power needed to transmit the higher frequencies is that required for aided tracking instead of the power needed for unaided acquisition. Thus, "bootstrapping" one's way up to the desired frequency results in a lower total power required in tracking a high frequency signal.

To help in deciding how to calculate the frequency intervals, a model must be created which accounts for the different contributions to the errors of the measured frequencies. The model is then examined to see how errors of the higher-frequency predictions vary with time and with

additional measurements. After this behavior has been modeled, a Kalman filter can be used to simulate the effects of real time measurements upon the state estimate covariances. Once we know how accurate our estimates will be for a particular set of frequencies, we can extrapolate our estimate of phase and frequency until we meet a pre-established criterion at the next highest frequency.

The basic measurements this system relies upon are those of phase and frequency. These observables have frequency dependent contributions from the system kinematics and the ionosphere. By kinematics we refer to the motions of the transmitter and the receiving satellite as well as the drift in the transmitter crystal oscillator and receiver data processor frequency source. The kinematic effect upon phase and its time derivatives (frequency, frequency drift rate, etc.) is directly proportional to frequency, whereas the ionospheric effect is inversely proportional to frequency. In equation form phase and phase rate appear, respectively, as

$$\phi = A f + B f^{-1} \quad \text{and} \quad \dot{\phi} = \dot{A} f + \dot{B} f^{-1} \quad (3,4)$$

State Space Model

The kinematic and ionospheric processes have different effects upon the two types of measurements as the frequency is varied. In order to investigate further, a state vector (\underline{x}) and measurement vector (\underline{y}) were defined as follows:

$$\underline{x}^T = [x_1 \dots x_6]^T = [A \quad \dot{A} \quad \ddot{A} \quad B \quad \dot{B} \quad \ddot{B}]^T \quad \underline{y} = [\phi_1 \quad \dot{\phi}_1] \quad (\text{measurements at one frequency})$$

The kinematic and ionospheric second time derivatives, \ddot{A} and \ddot{B} respectively, are modeled as Gauss-Markov processes. This choice reflects the assumption that these processes are random, but that their present values are exponentially correlated with past and future values with a time constant β^{-1} .

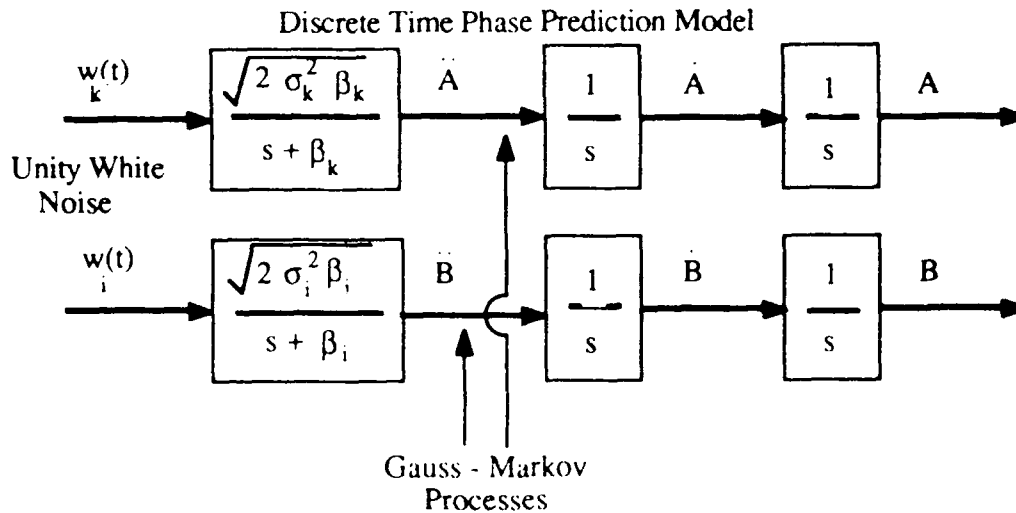


Figure 7. Integrated Gauss-Markov Processes

The state-space description of these processes is

$$\dot{\underline{x}} = F \underline{x} + G \underline{w} \quad \underline{y} = B \underline{x} \quad (5,6)$$

where F and the observation matrix B are given as

$$F = \begin{bmatrix} 0 & 1 & 0 \\ 0 & 0 & 1 \\ 0 & 0 & -\beta_k \end{bmatrix} \quad B = \begin{bmatrix} f_1 & 0 & 0 & f_1^{-1} & 0 & 0 \\ 0 & f_1 & 0 & 0 & f_1^{-1} & 0 \end{bmatrix} \text{ (again, measurements at one frequency)}$$

Since our measurement process is digital, we assume discrete measurements of phase and frequency taken at constant time intervals. The discrete time estimate of the state vector based on an estimate at a prior time can be made with the discrete state transition matrix (Φ_k).

$$\hat{A}_k = \Phi_{k-1} \hat{A}_{k-1} + w_{k-1} \quad (w_{k-1} \text{ is a process noise vector, } \neq w_k, w_i) \quad (7)$$

The entries of the discrete state transition matrix, Φ_k , can be calculated from the kinematic and ionospheric models from

$$\Phi_k = \left[L^{-1} [(sI - F)^{-1}] \right]_{t=\Delta t} = \begin{bmatrix} 1 & \beta t & b_k^{-2}(b_k \beta t - 1 + e^{-b_k \beta t}) \\ 0 & 1 & b_k^{-1}(1 - e^{-b_k \beta t}) \\ 0 & 0 & e^{-b_k \beta t} \\ 1 & \beta t & b_i^{-2}(b_i \beta t - 1 + e^{-b_i \beta t}) \\ 0 & 1 & b_i^{-1}(1 - e^{-b_i \beta t}) \\ 0 & 0 & e^{-b_i \beta t} \end{bmatrix} \quad (9)$$

The corresponding transfer functions and weighing functions between the kinematic and ionospheric process noises are obtained from the block diagrams. These weighing functions can now be integrated to derive the mean-square responses of the state variables to the process noises, the entries of the process covariance matrix.

Discrete Kalman Filter

For this study we are not interested with propagating estimates and making measurements to update the state vector. Instead, we are doing an analysis of the errors of the estimates of the state vector, the entries of the state estimate covariance matrix P_k . By iterating the Kalman filter covariance extrapolations and updates, the state covariance matrix should converge on a constant value after several measurements. After converging, the values of P_k can be used to calculate the next highest frequency which can accurately be acquired based on measurements at the lower frequencies. To start the filtering, *a priori* estimates of the state vector elements are used, based on previous information, such as prior measurements or crude estimates.

The system designer should consider two trials for finding the "bootstrapping" frequencies, one for a system which performs geodesy and vehicle tracking, and a second which performs geodetic measurements only.

For the first trial for vehicle tracking capabilities, vehicle dynamics will dominate the initial estimates of kinematic errors. The initial estimates for r.m.s. position, velocity, and acceleration errors are to be of the magnitude encountered when tracking a land vehicle, for example:

$$\sigma_A = 3.33(10^{-6}) \text{ s (corresponds to a 1000 m position uncertainty)}$$

$$\sigma_{\dot{A}} = 3.33(10^{-8}) \text{ (dimensionless) (corresponds to a } 10 \text{ m s}^{-1} \text{ velocity)}$$

$$\sigma_{\ddot{A}} = 3.33(10^{-8}) \text{ s}^{-1} \text{ (corresponds to a } 10 \text{ m s}^{-2} \text{ acceleration)}$$

Assumptions about ionospheric behavior are made (values below are referenced to 1 GHz):

$$\sigma_B = 3.33(10^{11}) \text{ Hz}^2 \text{ s (corresponds to 100 m pathlength uncertainty)}$$

$$\sigma_{\dot{B}} = 3.33(10^7) \text{ Hz}^2 \text{ (corresponds to a } 0.01 \text{ m s}^{-1} \text{ phase velocity)}$$

$$\sigma_{\ddot{B}} = 3.33(10^5) \text{ Hz}^2 \text{ s}^{-1} \text{ (corresponds to a } 10^{-4} \text{ m s}^{-2} \text{ frequency rate of change)}$$

The Gauss-Markov process noise variances and their time constants are also approximated:

$$\sigma_k^2 = 10^{-16} \text{ s}^{-2} \text{ (corresponds to a 0.3 g acceleration uncertainty)}$$

$$\sigma_i^2 = 1.1 \cdot (10^{11}) \text{ Hz}^4 \text{ s}^{-2} \text{ (corresponds to a } 10^{-4} \text{ m s}^{-2} \text{ frequency rate of change)}$$

$$\beta_k = 1.0 \text{ s}^{-1} \quad \beta_i = 0.1 \text{ s}^{-1}$$

A time interval between measurements (e.g., one second) needs to be selected, as well as the starting (lowest frequency) (e.g., 100 MHz).

For the second trial, for a system with only geodetic positioning capabilities, the ionospheric parameters remain the same. The kinematic mean error estimate of acceleration is no longer dependent upon the dynamics of the vehicle being tracked, but upon the oscillator stability. The time increments and starting frequency also remain the same. In this case the new estimates are:

$$\sigma_{\dot{A}} = 2.78(10^{-13}) \text{ s}^{-1} \text{ (corresponds to a } 10^{-9} \text{ oscillator frequency drift rate per hour)}$$

$$\sigma_{\ddot{A}} = 3.33(10^{-8}) \text{ (dimensionless) (corresponds to a } 10 \text{ m s}^{-1} \text{ velocity)}$$

$$\sigma_A = 3.33(10^{-6}) \text{ s (corresponds to a 1000 m position uncertainty)}$$

$$\beta_k = 1.39(10^{-4}) \text{ s}^{-1} \text{ (corresponds to two hours of continuous observation by any one satellite)}$$

The mean measurement errors (elements of R_k) are assumed to be independent between frequencies and independent between phase and frequency measurements at one transmitter frequency allocation. Therefore R_k is a diagonal matrix, and these diagonal entries are broken up into two regimes. At frequencies below 1 GHz the phase cannot be measured meaningfully due to ionospheric multipath. The assumed mean measurement error for frequency is

$$\sigma_{\dot{\phi}} = 0.2 \text{ Hz.}$$

At frequencies above 1 GHz, we assume that ionospheric multipath problems have diminished. However, independent measurements can only be obtained after one full integration time period has elapsed. In practice, however, correlated measurements are incorporated more frequently. To correct for this oversampling, the measurement covariances are corrected for the integration time it takes to obtain the measurement:

$$\sigma_{\phi} = 0.03 \cdot \sqrt{(\text{int.time})} \text{ cycles} \quad \sigma_{\dot{\phi}} = \frac{\sqrt{12}}{\text{Integration Time}} * \sigma_{\dot{\phi}} * (\text{int.time})^{3/2} = \sqrt{12} * \sigma_{\dot{\phi}} * \sqrt{(\text{int.time})}$$

Selecting New Frequencies

Since we assume that phase measurements are not useful at frequencies below 1 GHz, only the phase rate estimate accuracy is of concern in that regime. From the elements of Σ_k the frequency estimate variance can be written as a function of frequency:

$$\sigma_{\hat{\phi}}^2 = \sigma_{\hat{A}}^2 f^2 + 2 \sigma_{\hat{A}\hat{B}} + \sigma_{\hat{B}}^2 f^{-2} \quad (9)$$

Once the variances shown here have converged, this equation can be solved for the next highest frequency, given the criterion for the frequency variance at the next highest frequency:

$$\text{Below 1 GHz, } \sigma_{\hat{\phi}} = \frac{1 \text{ cycle}}{4 * \text{Integration Time}}$$

After phase and frequency measurements are being made at frequencies above 1 GHz, two criteria have to be met. In addition to the frequency relation, Σ_k yields an analogous phase variance equation and criterion:

$$\sigma_{\hat{\phi}}^2 = \sigma_{\hat{A}}^2 f^2 + 2 \sigma_{\hat{A}\hat{B}} + \sigma_{\hat{B}}^2 f^{-2} \quad (10)$$

Above 1 GHz, $\sigma_{\hat{\phi}} = 0.1$ cycles (to prevent cycle-slip error).

When predicting new frequencies above 1 GHz, both the phase and frequency predictions are made, and the lower frequency prediction is used. The measurement matrix (H_k) and the measurement covariance matrix (R_k) are enlarged to accommodate the additional phase and frequency measurements at the new transmitter frequency allocation.

In addition to these measurement criteria, the system designer can decide on other frequency allocations based on existing international frequency allocations. He still must meet the measurement criteria; that is, in order for the signal at the next highest frequency to be tracked, the measurements of the signals at all lower frequencies must meet the two conditions shown above.

Kalman Filter / Sample Frequency Selections

In the case of the vehicle tracking system, the uncertainty of the vehicle's acceleration from measurement to measurement, coupled with the time lag between measurements, limits the ability to predict signal phase and frequency at higher frequency allocations. Therefore the range of frequencies chosen is not as large as those chosen for the geodetic application. Even with this limitation, however, the bootstrapping technique can yield phase errors approaching one meter with only five frequencies. As shown in the table below, the bootstrapping technique yields smaller phase errors than are obtained with the lowest frequency alone. Also, bootstrapping consumes less power than is required to get the same accuracy by acquiring a signal at one higher frequency. The five frequencies together outperform the current proposal to use emergency locator transmitters at 405 MHz (case c).

For the case of the geodetic positioning system, it is possible to achieve a phase error on the order of one millimeter with seven frequencies. Table 2 shows the frequencies, the mean square errors achieved at each frequency, and the total power needed to broadcast at these frequencies.

(a)	Bootstrap Frequency (MHz)	Std. Dev. Phase (m)	Std. Dev. Freq. (m/s)	Peak Power (w)
1	100.0	2.21	0.21	0.80
2	109.9	1.62	0.20	0.78
3	134.1	1.13	0.19	0.73
4	156.2	1.29	0.19	0.70
5	176.2	1.50	0.20	0.67

TOTAL POWER TRANSMITTED: ~ 3.7watts

(b)	Bootstrap Frequency (MHz)	Std. Dev. Phase (m)	Std. Dev. Freq. (m/s)	Peak Power Transmitted
1	100.0	10.6	0.60	<u>0.8 watts</u>

(c)	Bootstrap Frequency (MHz)	Std. Dev. Phase (m)	Std. Dev. Freq. (m/s)	Peak Power Transmitted
1	405.0	2.62	0.15	<u>8.5 watts</u>

Table 1. FREQUENCY SELECTIONS, MEAN ERRORS AND REQUIRED POWER FOR (a) VEHICLE POSITIONING SYSTEM; (b) FOR '100 MHZ ONLY' SYSTEM; (c) FOR 405 MHZ SAR SYSTEM.

	Bootstrap Frequency	Standard Dev. of Phase Estimate (mm)	Standard Dev. of Frequency Est. (mm/s)	Signal Power (w)
1	100 MHz	1040.	99.6	0.80
2	129.5 MHz	619.	59.4	0.74
3	557.9 MHz	32.9	3.19	0.48
4	1.13 GHz	7.79	0.773	0.39
5	2.06 GHz	2.60	0.261	0.32
6	4.44 GHz	1.69	0.145	0.38
7	8.97 GHz	1.72	0.141	1.10

PEAK POWER TRANSMITTED: ~ 4.21watts

Table 2. GEODETIC SYSTEM.FREQUENCY SELECTIONS, MEAN ERRORS, AND REQUIRED POWER

Note that in both the vehicle and geodetic cases, the second lowest frequency is very close in value to the lowest frequency, the reason being that measurements at one frequency alone cannot separate the kinematic and ionospheric contributions to the phase and frequency measurements. Once measurements are simultaneously taken at the two lowest frequencies, the new information about the two processes drives down the state vector covariances by several orders of magnitude, enabling the third lowest frequency to be located further up the electromagnetic spectrum.

(a)	# of Frequencies	Highest Frequency (MHz)	$\sigma_{\hat{A}}$ (dimensionless)	$\sigma_{\hat{B}}$ (GHz ²)
	1	100.0	3.87(10 ⁻⁹)	3.32(10 ⁻¹¹)
	2	110.0	1.71(10 ⁻⁹)	1.20(10 ⁻¹¹)
	3	136.1	1.15(10 ⁻⁹)	7.82(10 ⁻¹²)
	4	158.4	8.76(10 ⁻¹⁰)	6.31(10 ⁻¹²)
	5	178.5	7.07(10 ⁻¹⁰)	5.57(10 ⁻¹²)

(b)	# of Frequencies	Highest Frequency (MHz)	$\sigma_{\hat{A}}$ (dimensionless)	$\sigma_{\hat{B}}$ (GHz ²)
	1	100.0	3.37(10 ⁻⁹)	3.33(10 ⁻¹¹)
	2	130.4	8.26(10 ⁻¹¹)	4.07(10 ⁻¹²)
	3	800.7	1.95(10 ⁻¹¹)	3.94(10 ⁻¹²)
	4	2300.	2.24(10 ⁻¹²)	3.62(10 ⁻¹²)
	5	4970.	1.09(10 ⁻¹²)	3.42(10 ⁻¹²)

Table 3. IMPROVEMENT OF STATE ESTIMATES WITH ADDITIONAL FREQUENCIES
(A) VEHICLE TRACKING CASE, (B) GEODETIC CASE

(Note: Estimates of \hat{A} and \hat{B} are shown instead of A and B since only frequency measurements were being performed at lower ($f < 1\text{GHz}$) frequencies.)

CONCLUSIONS

It is possible to design a relay satellite constellation which can accommodate low power (~ 1.0 w) SAR and geodetic radio transmitters. By defining user positioning requirements one can perform an analysis of the radio spectrum to find candidate frequency allocations for a new system. There is a (growing) need to measure and control the effects of interfering man-made radio noise in space, as well as a need to study the possibilities of suitable frequency allocation sharing among different radio applications.

In addition to estimating the required uplink power, an algorithm has been shown which can be used to select transmitter frequencies which will maximize the positioning capability of the GeoBeacon transmitter. With simple models of the man-made electromagnetic noise environment in high earth orbits and of ionospheric behavior, a system designer can use a Kalman filter to make choices as to the most advantageous frequency allocations for this system. The Kalman filter can be used make frequency selections over a variety of levels of positioning accuracy; thus, this methodology for frequency selection can accommodate different user needs as well as man - made frequency allocation restrictions.

RECOMMENDATIONS

Improved Radio Noise and Interference Models

As demonstrated earlier, the piece of information with the greatest uncertainty is the noise temperature estimate from man-made noise (incidental and transmitter) from the Earth as seen from Earth orbit. This estimate would vary with altitude, frequency, weather, local time of day, and season. The ITU (International Telecommunications Union) has already foreseen this need and

has issued recommendations for "propagation data required for the design of Earth-space telecommunication systems..." and "propagation data required for the evaluation of interference between stations in space and those on the surface of the Earth..."³ The results of this study reinforce the need for these recommendations to be acted upon as soon as possible.

In addition, as more useful radio systems vie for a finite number of frequency allocations, it will become more important to have accurate measurements of the levels of interference which can be expected from other systems sharing the allocation. These measurements will need to be made at a variety of orbit altitudes in addition to the Earth's surface.

Improved Ionospheric Multipath Model

There is a need to understand the relations between ionospheric multipath scintillations and frequency. Once the expected phase change can be modeled as a function of frequency, the effects of measurements at lower frequencies in the Kalman filter can aid in the prediction of multipath effects at other frequencies.

AMSAT/OSCAR Experiment

Over the last 20 years, amateur radio operators have launched several OSCAR (Orbiting Satellite Carrying Amateur Radio) repeater satellites into Earth orbit. Two OSCAR satellites, designated AO-10 and AO-13, are in highly elliptic inclined orbits (~4000 km by ~35000 km) which occasionally allows for continuous observation times on the order of several hours. The satellites' uplink frequencies could be used to perform crude baseline measurements with transmitters similar to those developed in this study.

ACKNOWLEDGEMENTS

The author completed this work while supported by a Minority Fellowship from the National Science Foundation (with tenureship covering the 1987-1990 academic years.) Work done with the Space Geodesy Group of the Center for Space Research was made possible by Air Force Contract F19628-86-K-0009 with the Air Force Geophysics Laboratory.

REFERENCES

1. Agrawal, Brij N., *Design of Geosynchronous Spacecraft*, Prentice-Hall, Inc., Englewood Cliffs, NJ, 1986.
2. Battin, Richard H., *An Introduction to the Mathematics and Methods of Astrodynamics*, AIAA Ed. Series, 1987.
3. CCIR, Report 396-5, Annex VI, "Maintenance Telemetry, Tracking, and Telecommand for Developmental and Operational Satellites," in Volume II, *Recommendations and Reports of the CCIR*, 1986, pp. 158 - 170, International Telecommunications Union, Geneva, 1986.
4. Counselman, III, Charles C. and Gourevitch, Sergei A., "Miniature Interferometer Terminals for Earth Surveying: Ambiguity and Multipath with Global Positioning System," *IEEE Transactions on Geoscience and Remote Sensing*, Vol. GE-19, No.4, October 1981.
5. Crane, R.K., "An Algorithm to Retrieve Water Vapor Information from Satellite Measurements," NEPRF Tech. Rept. 7-76 (ERT) Final Report, Project No. 1423, Environmental Research and Technology, Inc., November 1976.
6. Davidoff, Martin R., *The Satellite Experimenter's Handbook*, American Radio Relay League, Newington, CT, 1985.
7. Gelb, Arthur, *Applied Optimal Estimation*, MIT Press, Cambridge, MA, 1974.
8. Herman, J. R., "The Radio Noise Environment in Near Space: A Review," *Proc. IEEE International Symposium on Electromagnetic Compatibility*, June 20 - 22, 1978.

9. Herring, Thomas A., notes from a presentation given at MIT, October 26, 1988.
10. Ippolito Jr., Louis J., *Radiowave Propagation in Satellite Communications*, Van Nostrand Reinhold Company, New York, 1986.
11. *ITU Radio Regulations*, International Telecommunication Union, Geneva, 1982.
12. King, R. W., Masters, E. G., Rizos, C., Stolz, A., and Collins, J., *Surveying With GPS*, Monograph 9, School of Surveying, The University of New South Wales, Kensington, N.S.W. Australia, 1985.
13. Skomal, Edward N., "Analysis of Spaceborne VHF Incidental Noise Over the Western Hemisphere," *IEEE Transactions on Electromagnetic Compatibility*, Vol. EMS-25, No. 3, August 1983, pp. 321-328.
14. Skomal, E. N. and Smith, A. A., *Measuring the Radio Frequency Environment*, Van Nostrand Reinhold Company, New York, 1985.
15. Smith, Ernest K. and Njoku, Eni G., "The Microwave Noise Environment at a Geostationary Satellite Caused by the Brightness of the Earth," *Symposium Record - IEEE 1985 International Symposium on Electromagnetic Compatibility*, August 20-22, 1985.
16. Spilker Jr., J.J., "GPS Signal Structure and Performance Characteristics," *Global Positioning System, Navigation, Journal of the Institute of Navigation*, Vol. 25, No. 2, 1978.
17. van Graas, Frank, "Sole Means Navigation Through Hybrid Loran-C and GPS," *Navigation: Journal of the Institute of Navigation*, Vol. 35, No. 2, Summer 1988.
18. Wells, David, *Guide to GPS Positioning*, Canadian GPS Associates, Fredericton, N.B., Canada, 1986.
19. Wenzel, R. J., "Omega Navigation System - A Status Report," *Navigation: Journal of the Inst. of Navigation*, Vol. 35, No. 3, Fall 1988.